Primate lentiviruses are differentially inhibited by interferon-induced transmembrane proteins

Jin Qian [a,b,1], Yann Le Duff [a,1], Yimeng Wang [a,b], Qinghua Pan [a], Shilei Ding [a,c], Yi-Min Zheng [d], Shan-Lu Liu [d], Chen Liang [a,b,c,*]

[a] Lady Davis Institute, Jewish General Hospital, Montreal, Quebec, Canada H3T 1E2
[b] Department of Medicine, McGill University, Montreal, Quebec, Canada H3A 2B4
[c] Department of Microbiology and Immunology, McGill University, Montreal, Quebec, Canada H3A 2B4
[d] Department of Molecular Microbiology & Immunology, School of Medicine, Bond Life Sciences Center, University of Missouri, Columbia, MO 65211-7310, USA

ARTICLE INFO

ABSTRACT

Interferon-induced transmembrane (IFITM) proteins inhibit the entry of a large number of viruses. Not surprisingly, many viruses are refractory to this inhibition. In this study, we report that different strains of HIV and SIV are inhibited by human IFITM proteins to various degrees, with SIV of African green monkeys (SIV$_{AGM}$) being mostly restricted by human IFITM2. Interestingly, SIV$_{AGM}$ is as much inhibited by human IFITM2 as by IFITM3 of its own host African green monkeys. Our data further demonstrate that the entry of SIV$_{AGM}$ is impaired by human IFITM2 and that this inhibition is overcome by the cholesterol-binding compound amphotericin B that also overcomes IFITM inhibition of influenza A viruses. These results suggest that IFITM proteins exploit similar mechanisms to inhibit the entry of both pH-independent primate lentiviruses and the pH-dependent influenza A viruses.

Introduction

Interferon-induced transmembrane (IFITM) proteins inhibit a wide range of viruses (reviewed in (Diamond and Farzan, 2013; Perreira et al., 2013)). Humans have five IFITMs including IFITM1, 2, 3, 5 and 10 among which IFITM1, 2 and 3 exhibit antiviral activities (Hickford et al., 2012). These three IFITMs are ubiquitously expressed in different tissues, and respond to type I interferon stimulation. IFITM5 is strictly expressed in osteoblasts and has a role in bone mineralization (Moffatt et al., 2008). The function of IFITM10 remains unknown. Many important human pathogenic viruses are sensitive to IFITM restriction. These include influenza A virus, flaviviruses, Ebola virus, SARS coronavirus, Rift Valley fever virus, reovirus, human immunodeficiency virus type 1 (HIV-1), etc. (Anafu et al., 2013; Brass et al., 2009; Huang et al., 2011; Jiang et al., 2010; Lu et al., 2011; Mudhasani et al., 2013). The importance of IFITM proteins in host antiviral defense is demonstrated by the high mortality of *ifitm*3-knockout mice infected with influenza A

virus and by the possible association of an SNP in the human *ifitm*3 gene with the disease severity caused by influenza virus infection (Bailey et al., 2012; Everitt et al., 2012; Wakim et al., 2013; Zhang et al., 2013).

IFITMs are small transmembrane proteins containing 120 to 135 amino acids (Siegrist et al., 2011). IFITM2 and 3 share higher homology as compared to IFITM1, which has a relatively shorter N-terminal region and a longer C-terminal region. IFITM proteins have two predicted transmembrane (TM) domains. However, recent data suggest that only the C-terminal TM domain of IFITM3 crosses the membrane, whereas the N-terminal one serves as an intramembrane domain (IMD) (Bailey et al., 2013; Jia et al., 2012; Yount et al., 2012). This IMD likely associates with the cytoplasmic leaflet of the lipid bilayer with the help of palmitoylated cysteine residues (Yount et al., 2012). This type of membrane topology allows the cytoplasmic exposure of a large portion of IFITM sequences that may interact with cellular factors and machineries that collectively modulate the functions of IFITMs. One example is the 20-YEML-23 motif of IFITM3 that interacts with the adaptor protein AP-2 and regulates IFITM3 endocytosis from the plasma membrane en route to late endosomes (Chesarino et al., 2014; Jia et al., 2012). The K24 residue of IFITM3 is a major site of ubiquitination. This modification affects IFITM3 subcellular localization and antiviral activity (Yount et al., 2012).

The IFITM proteins inhibit virus infection by impairing virus entry (Feeley et al., 2011). Two models of inhibition have been proposed. One model suggests that IFITM proteins interfere with membrane hemifusion (Li et al., 2013). This model is supported by the results that IFITM proteins suppressed cell membrane hemifusion that was created by low pH at cold temperature. This inhibition was rescued by oleic acid that promotes membrane hemifusion (Li et al., 2013). The second model proposes that IFITM proteins impede the formation of viral fusion pore (Desai et al., 2014). In support of this latter model, no effect was detected on lipid mixing between viral membrane and endosomal membrane upon IFITM3 overexpression. Yet, the release of viral genome into the cytoplasm was blocked by IFITM3 (Desai et al., 2014). Both models are consistent with the notion that IFITM proteins can modulate the biophysical property of lipid bilayer, such as membrane fluidity and curvature, through mechanisms that possibly involve the interaction of IFITMs with VAPA and the disruption of intracellular cholesterol homeostasis (Amini-Bavil-Olyaee et al., 2013). In support of this mechanism, a cholesterol-binding agent amphotericin B overcomes the inhibition of influenza A virus infection by IFITM3 (Lin et al., 2013).

Not all enveloped viruses are inhibited by IFITM proteins. Examples are lymphocytic choriomeningitis virus (LCMV), Lassa virus (LASV), Machupo virus (MACH), human papillomavirus, cytomegalovirus and adenovirus that are all resistant to IFITMs (Brass et al., 2009; Warren et al., 2014). Among retroviruses, murine leukemia virus (MLV) is relatively refractory to IFITMs, the HIV-1 strain BH10 is inhibited, whereas another HIV-1 strain IIIB exhibits resistance (Brass et al., 2009; Lu et al., 2011). In this study, we examined a panel of HIV and SIV strains for their sensitivity to IFITM inhibition. The results revealed various degrees of inhibitions ranging from no inhibition for HIV-1$_{A/G}$ to 10-fold inhibition for SIV of African green monkeys.

Results

IFITM proteins inhibit primate lentiviruses

In order to evaluate the susceptibility of different primate lentiviruses to inhibition by IFITM1, 2 and 3, we selected the following viruses for study, including three HIV-1 strains (the laboratory adapted strain NL4-3, primary isolate YU-2 and the circulating recombinant form A/G), one HIV-2 strain (HIV-2$_{Rod}$), five SIV strains from chimpanzees (SIV$_{CPZ1.9}$), African green monkeys *Chlorocebus sabaeus* (SIV$_{AGM-sab}$) and *Chlorocebus tantalus* (SIV$_{AGM-tan}$), rhesus macaques (SIV$_{MAC-1A11}$) and sooty mangabeys (SIV$_{SMM}$). Since these viruses either use CXCR4 or CCR5 as the co-receptor, we chose to infect the HIV indicator cell line TZM-bl that expresses both CXCR4 and CCR5 and are thus susceptible to infection by all these viruses. We first transduced TZM-bl cells with retroviral vectors expressing human IFITM1, 2 or 3 and selected the stably transduced cell lines with puromycin. Ectopic expression of IFITM1, 2 and 3 was confirmed by western blotting (Fig. 1A). We then challenged these TZM-bl cell lines with different doses of HIV or SIV. Virus infection was monitored by measuring luciferase activity that was expressed under the control of HIV-1 LTR promoter in TZM-bl cells. The data report the effect of IFITM proteins on the early phase of HIV/SIV infection until viral Tat protein is produced. Fig. 1B shows the luciferase activities of one representative infection experiment that was performed with different doses of viruses. The averages of three independent experiments are summarized in Fig. 1C. The results showed that SIV$_{AGM-tan}$ was inhibited the most, whereas infection of HIV-1, SIV$_{CPZ1.9}$ and SIV$_{MAC}$ were not profoundly affected by the three human IFITM proteins. On the basis of the degrees of inhibition,

these primate lentiviruses are ranked as SIV$_{AGM-tan}$ > SIV$_{AGM-sab}$, SIV$_{SMM}$, HIV-2$_{Rod}$ > HIV-1$_{NL4-3}$, HIV-1$_{YU-2}$, HIV-1$_{A/G}$ > SIV$_{CPZ1.9}$ and SIV$_{MAC}$. The results also revealed that IFITM2 was the most inhibitory, followed by IFITM3 and IFITM1.

IFITM2 strongly diminishes the entry of SIV$_{AGM}$

Since IFITM proteins are known to inhibit virus entry (Feeley et al., 2011; Lu et al., 2011), we asked whether the strong inhibition of SIV$_{AGM}$ by IFITM2 is a result of impaired virus entry. To this aim, we prepared the BlaM-Vpr-containing HIV and SIV particles, and used these virions to infect IFITM-expressing TZM-bl cells. The efficiency of virus entry was determined by measuring the cleavage of CCF2 by BlaM-Vpr that enters the cytoplasm together with viral cores. The results showed that the entry of HIV-1$_{NL4-3}$ and SIV$_{MAC}$ into TZM-bl was marginally affected by IFITM1, 2 or 3 (Fig. 2). In contrast, the entry of SIV$_{AGM-tan}$ and SIV$_{AGM-sab}$, to a lesser extent SIV$_{SMM}$, was strongly impaired by IFITM2 and IFITM3 (Fig. 2). This similar reduction in the entry of SIV$_{AGM-tan}$ and SIV$_{AGM-sab}$ contrasts with a moderately stronger inhibition of SIV$_{AGM-tan}$ infection by IFITM2 and 3 as shown in Fig. 1. This difference suggests that SIV$_{AGM-tan}$ may be inhibited not only at the entry step, but also at a downstream step until viral Tat is produced, which is measured in the assays shown in Fig. 1.

We next asked whether the endogenous IFITM2 and 3 are able to inhibit the entry of SIV$_{AGM}$. We first used shRNA to knock down IFITM2 and 3 in TZM-bl cells (Fig. 3A). Both SIV$_{AGM-tan}$ and SIV$_{AGM-sab}$ showed significantly higher infection in the IFTIM2/3-knockdown cells (Fig. 3B). Since the BlaM-Vpr containing SIV$_{AGM-sab}$ particles generated much stronger signals in the entry assay than SIV$_{AGM-tan}$ (Fig. 2), we further measured the effect of IFITM2/3-knockdown on the entry of SIV$_{AGM-sab}$. We also treated TZM-bl cells with IFNα2b to increase the expression of endogenous IFITM2 and 3. The results showed that IFNα2b reduced the entry of SIV$_{AGM-sab}$ by 2-fold and this diminution was completely lost when IFITM2 and 3 were depleted with shRNA (Fig. 3C and D). When the endogenous IFITM2 and 3 were knocked down in a human T cell line called C8166 that constitutively express relatively high level of IFITM2, the entry of SIV$_{AGM-sab}$ increased by approximately 50% (Fig. 3E–G). IFNα2b treatment increased the expression of IFITM2 and 3, and results in a 40% reduction in SIV$_{AGM-sab}$ entry. Depletion of IFITM2 and 3 under IFNα2b treatment restored SIV$_{AGM-sab}$ entry to the control level (Fig. 3E and F). We also observed that shRNA3 depleted IFITM2 much more efficiently compared to shRNA1 and shRNA2 (Fig. 3E), which correlates with a moderately greater entry of SIV$_{AGM-sab}$ in shRNA3-transdued C8166 cells than in shRNA1- or shRNA2-transduced cells, albeit that this increase does not reach statistical significance (Fig. 3F and G). Together, these data indicate that endogenous IFITM2 and 3 inhibit the entry of SIV$_{AGM-sab}$.

Amphotericin B overcomes the inhibition of SIV$_{AGM}$ by IFITM2 and 3

It has been reported that amphotericin B prevents IFITM3 from inhibiting influenza A virus through modulating membrane fluidity (Lin et al., 2013). We suspected that, if IFITM2 and 3 use the same mechanism to inhibit SIV$_{AGM}$ and influenza A virus, then amphotericin B should also rescue the infection of SIV$_{AGM}$ in IFITM2/3-expressing cells. Indeed, when amphotericin B was added with increasing doses, the infection of both SIV$_{AGM-sab}$ and SIV$_{AGM-tan}$ in IFITM2 or IFITM3-expressing TZM-bl cells were restored to the level of infection in control cells (Fig. 4A and B). HIV and SIV are known as pH-independent viruses (McClure et al., 1988). Yet, the high sensitivity of SIV$_{AGM}$ to IFITM2 and 3 inhibition raises the possibility that this SIV may have become pH-dependent similar to the influenza A virus. Contrary to this speculation, SIV$_{AGM}$ showed resistance to the treatment of chloroquine or bafilomycin A1 both of which neutralize
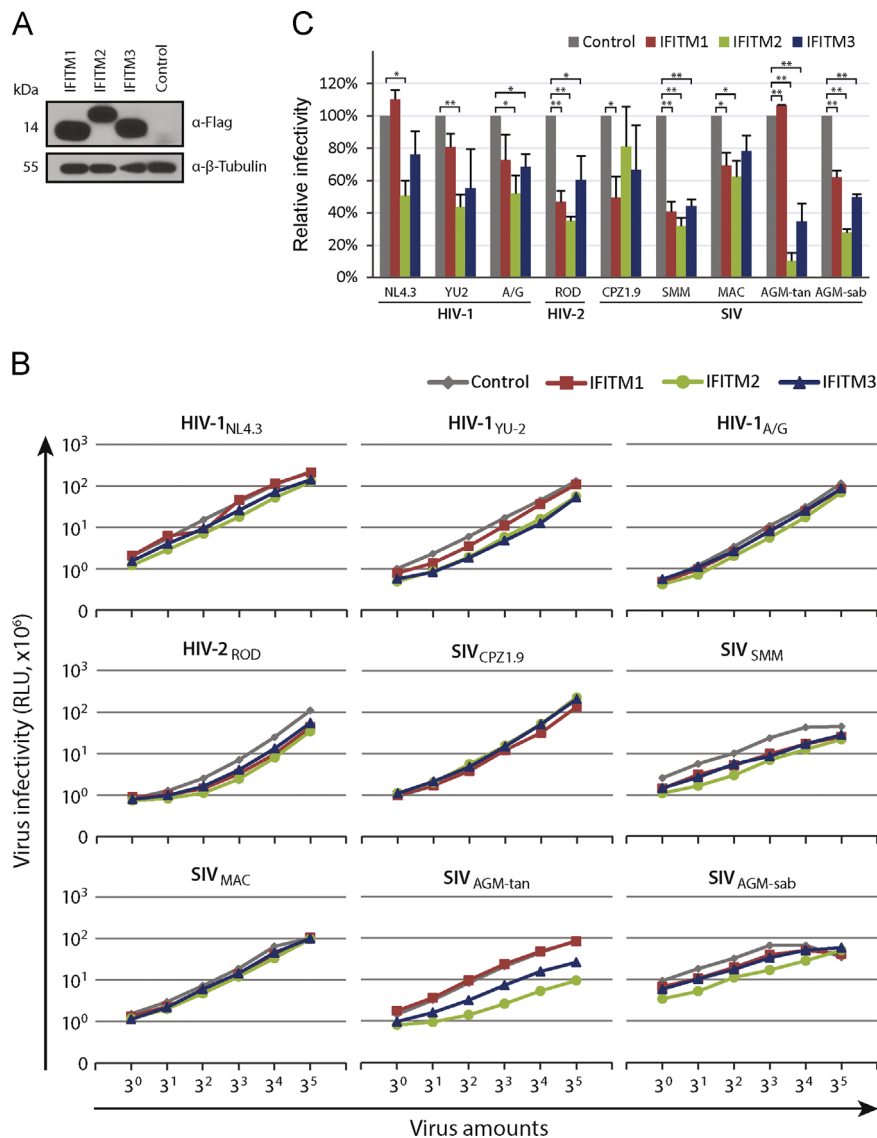
Fig. 1. Effects of human IFITM1, 2 and 3 on infection of HIV and SIV. (A) TZM-bl cells were stably transduced with IFITM1, 2 or 3. Each IFITM has a Flag tag at the N-terminus. Expression levels of IFITMs were determined by western blotting. Control represents cells that were transduced with empty retroviral vector pQCXIP. (B) Infection of TZM-bl cell lines with HIV and SIV. Three HIV-1 strains (NL4-3, YU-2 and A/G), one HIV-2 strain (ROD), five SIV strains (CPZ1.9, SMM, MAC, AGM-tan and AGM-sab) were utilized in infections. For each virus, series of five dilutions were tested. The virus amounts were chosen to generate infectivity in the linear range. Results shown represent the data of three independent experiments. (C) Summary of three independent experiments at the infection dose of 3^3 for all tested viruses. The infection of the control TZM-bl cells is arbitrarily set as 100% for each virus. Student's t-tests were performed to calculate the p-Values. The p-Values were presented as * ($p < 0.05$) or ** ($p < 0.01$).

the pH in late endosomes and thus inhibit VSV G protein-mediated pH-dependent virus entry (Fig. 4C). In further support of this observation, the dynamin inhibitor dynasore moderately stimulated the infection of SIV_{AGM} (Fig. 4D), which suggests that, in contrast to VSV that enters the cell via endocytosis and is thus sensitive to dynasore treatment, the entry of SIV_{AGM} is independent of endocytosis. Together, these data indicate that IFITM2 and 3 exploit a similar mechanism to inhibit viruses that enter cells via different pathways.

SIV_{AGM} is strongly restricted by IFITM3 of African green monkeys

We next asked whether SIV_{AGM} is inhibited by IFITM proteins of its natural host, African green monkeys. To answer this question, we first cloned IFITM1 and IFITM3 from the African green monkey kidney cell lines called COS-7 and Vero. The agmIFITM1 exhibits a much higher homology to macaque IFITM1 than to IFITM1 of humans and chimpanzees (Fig. 5A). Similar to human IFITM1, agmIFITM1

exhibited no or only weak inhibition of HIV or SIV (Fig. 5B). Four agmIFITM3 sequences were identified that differ at amino acid positions 22 and 38 (Fig. 5A), no distinct agmIFITM2 sequence was found. All four agmIFITM3 proteins inhibited HIV and SIV, with $SIV_{AGM-tan}$ and $SIV_{AGM-sab}$ being the most inhibited (Fig. 5B). The agmIFITM3 appears to elicit a much stronger inhibition than human IFITM2 or IFITM3 (Fig. 1), which might have enabled agmIFITM3 to suppress the infection of $SIV_{AGM-tan}$ and $SIV_{AGM-sab}$ to similar low levels. The differences at amino acid positions 22 and 38 affected the antiviral activity of IFITM3, agmIFITM3(I22H38) elicited the strongest inhibition (Fig. 5B). Notably, the I22 residue is located within the 20-YEML-23 motif that directs the endocytosis of human IFITM3 (Chesarino et al., 2014; Jia et al., 2012; Jia et al., 2014). This may explain the effect of M22I change on the antiviral function of agmIFITM3. Since SIV_{AGM} is potently inhibited by both human IFITM2 and agmIFITM3, it is likely that SIV_{AGM} is much more susceptible to IFITM restriction than other HIV and SIV strains regardless of the species origin of the IFITM proteins.
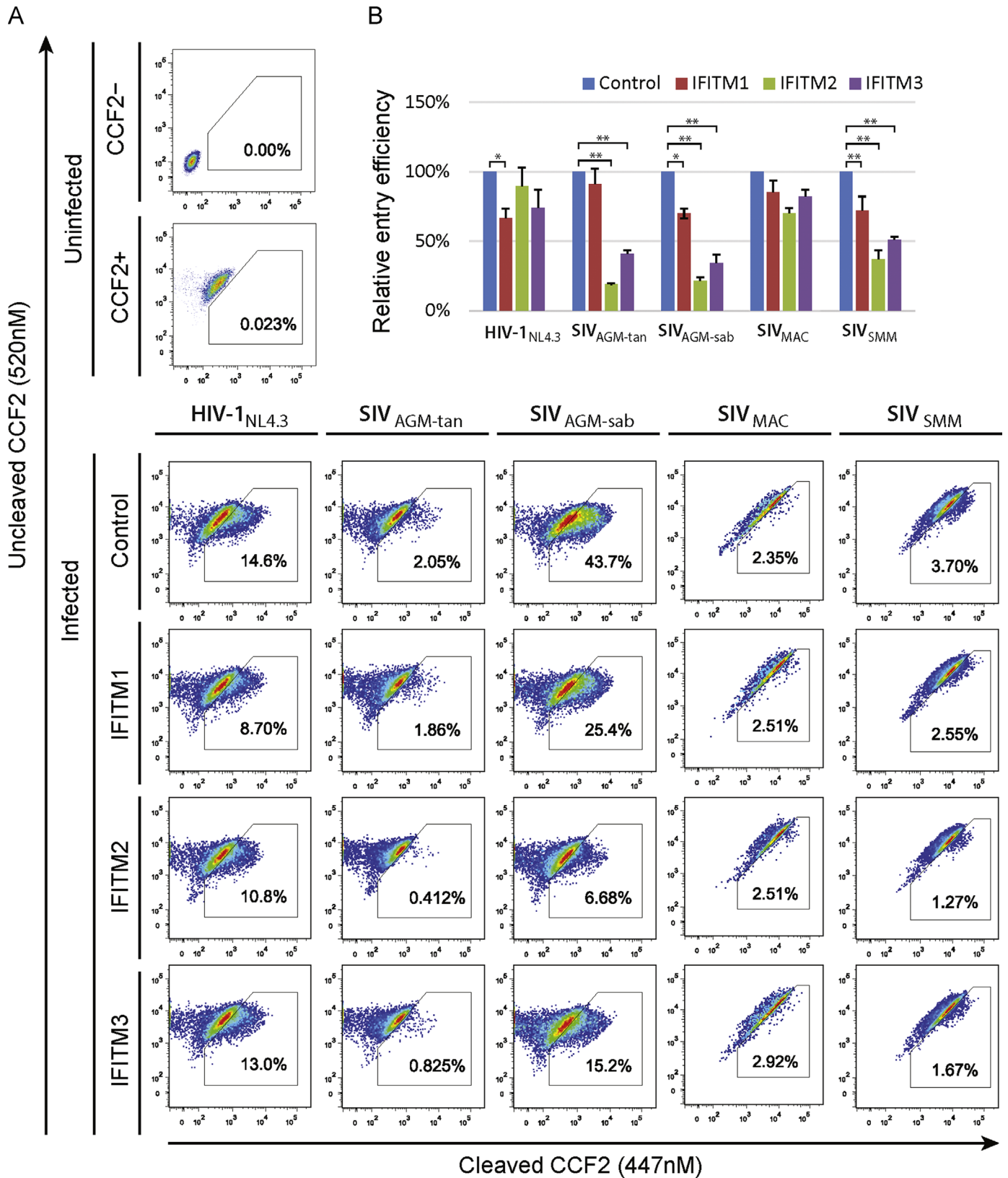
Fig. 2. Effects of human IFITM1, 2 and 3 on HIV and SIV entry. (A) The BlaM-Vpr-containing viruses were produced by transfecting HEK293T cells with pBlaM-Vpr DNA and each of the HIV-1$_{NL4.3}$, SIV$_{AGM-tan}$, SIV$_{AGM-sab}$, SIV$_{MAC}$ or SIV$_{SMM}$ DNA. These viruses were then used to infect TZM-bl cell lines that stably express IFITM1, 2 or 3. Virus entry was determined by measuring the cleavage of CCF2 by BlaM-Vpr. (B) Results of three independent experiments are summarized. Virus entry of the control cells is arbitrarily set as 100%. The p-Values were calculated and are presented as * ($p < 0.05$) or ** ($p < 0.01$).
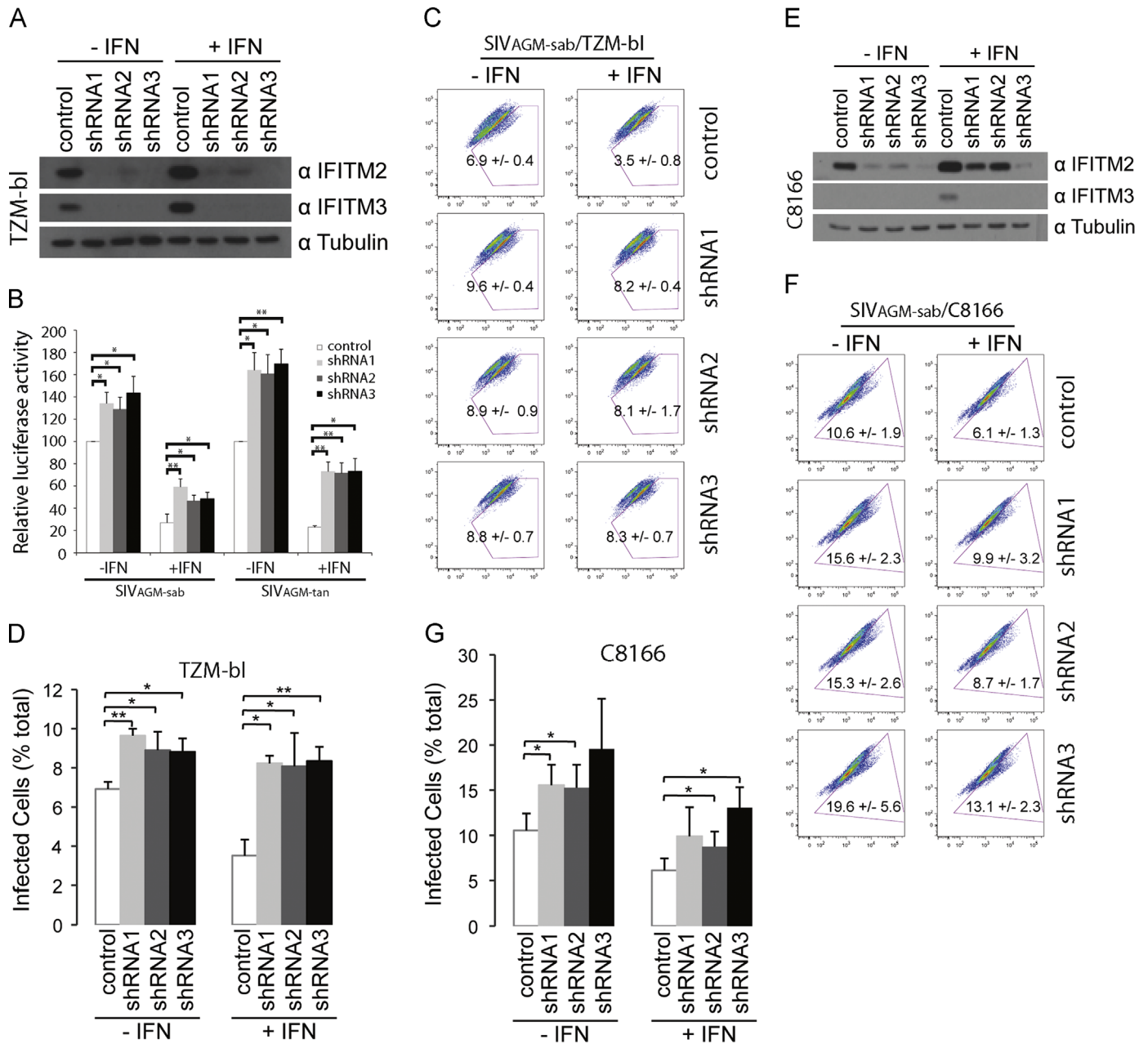
Fig. 3. Knockdown of endogenous IFITM2 and 3 increases the entry of SIV$_{AGM-sab}$. (A) Knockdown of endogenous IFITM2 and 3 in TZM-bl cells. Three shRNA clones targeting both IFITM2 and 3 were transduced into TZM-bl cells with or without IFNα-2b treatment (1000 U/ml, 16 h). Levels of endogenous IFITM2 and 3 were assessed by Western blotting. (B) Effect of endogenous IFITM2 and 3 on the infection of SIV$_{AGM-sab}$ and SIV$_{AGM-tan}$. IFITM2/3-knockdown TZM-bl cells were first treated with IFNα-2b and then infected with SIV$_{AGM-sab}$ or SIV$_{AGM-tan}$. Viral infection was determined by measuring luciferase activities in the infected TZM-bl cells. Results of three independent experiments are summarized in the bar graph with the infection of control TZM-bl cells arbitrarily set as 100%. (C) Effect of endogenous IFITM2 and 3 on SIV$_{AGM-sab}$ entry in TZM-bl cells. BlaM-Vpr-containing SIV$_{AGM-sab}$ was used to infect the IFITM2/3-knockdown TZM-bl cells. Levels of virus entry were assessed by measuring the cleavage of CCF2 using flow cytometry. (D) The results of three independent virus entry experiments are summarized in the bar graph. (E) Knockdown of endogenous IFITM2 and IFITM3 in C8166 cells. The knockdown efficiency was examined by western blotting. (F and G) Effect of endogenous IFITM2 and 3 in C8166 cells on SIV$_{AGM-sab}$ entry. Details refer to the legend to (C) and (D). The pValues were calculated and are presented as * ($p < 0.05$), ** ($p < 0.01$).

Discussion

Viruses of different families are affected by IFITM proteins to various degrees. Some viruses are strongly inhibited, examples are influenza A viruses, flaviviruses, Ebola viruses, and SARS coronaviruses (Brass et al., 2009; Huang et al., 2011). Some are moderately inhibited, such as vesicular stomatitis virus (Weidner et al., 2010). Some are resistant to IFITM, including LCMV, MACH, LASV, MLV, papillomavirus, cytomegalovirus and adenovirus (Brass et al., 2009; Warren et al., 2014). Infection of human coronavirus OC43 is even stimulated by IFITM2 or 3 (Zhao et al., 2014). Results of our

study showed that members of the same virus family such as lentiviruses can be affected by IFITM proteins to markedly different degrees that range from virtually no inhibition of SIV$_{CPZ1.9}$ and SIV$_{MAC}$ to a 10-fold restriction of SIV$_{AGM}$ by human IFITM2.

This observation appears to mirror the species-specific antiviral activity that has been described for some host restriction factors such as tetherin (Sauter et al., 2009). Human tetherin does not inhibit HIV-1 because of the countering action of viral antagonist Vpu, but it can block the release of SIV$_{AGM}$. In a similar vein, African green monkey tetherin potently inhibits HIV-1 owing to the inability of HIV-1 Vpu to antagonize this monkey tetherin.
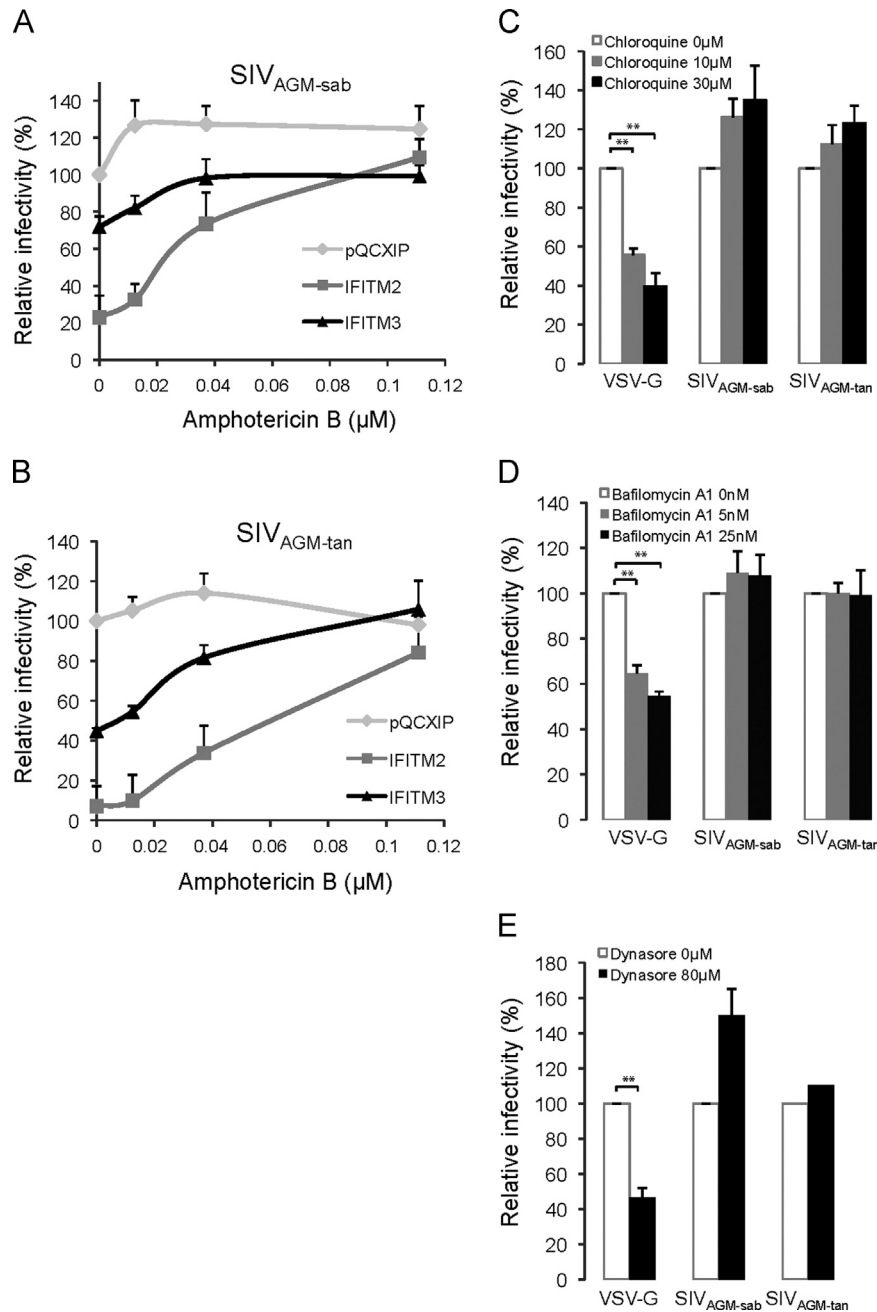
Fig. 4. Effects of different agents on SIV infection. (A and B) Different doses of amphotericin B were used to treat TZM-bl cell lines that stably express IFITM2 and 3. The control cell line was transduced with the empty pQCXIP retroviral vector. After one-hour pretreatment, cells were infected with SIV$_{AGM-sab}$ (A) or SIV$_{AGM-tan}$ (B). Virus infection was monitored by measuring luciferase activity in TZM-bl cell lysates. (C and D) TZM-bl cells were treated with different doses of chloroquine or bafilomycin A1 to neutralize the low pH in late endosomes and lysosomes. Cells were infected with SIV$_{AGM-sab}$, SIV$_{AGM-tan}$ or VSV-G pseudotyped HIV-1$_{NL4-3}$. Virus infection was determined by measuring luciferase activity in TZM-bl cell lysates. (E) TZM-bl cells were treated with or without dynasore for 1 h followed by infection with SIV$_{AGM-sab}$, SIV$_{AGM-tan}$ or VSV-G pseudotyped HIV-1$_{NL4-3}$. Levels of virus infection were monitored by measuring luciferase activity in TZM-bl cell lysates. Results shown are the averages of three independent experiments. The p-Values were calculated and are presented as ** ($p < 0.001$).

However, our results showed that agmIFITM3 inhibits SIV$_{AGM}$ more potently than human IFITM2 does, which suggests that SIV$_{AGM}$ may have not been sufficiently pressured to escape from the agmIFITM3 restriction. It is known that, in contrast to HIV and SIV infections that cause AIDS, SIV$_{AGM}$ or SIV$_{SMM}$ infection of their natural hosts is not pathogenic, which is at least partially attributable to the rapid resolution of innate immune responses at the acute infection stage and the lack of chronic immune activation (Harris et al., 2010; Jacquelin et al., 2014). Therefore, after establishing the infection, SIV$_{AGM}$ or SIV$_{SMM}$ does not face the inhibition by interferon and ISGs including IFITM proteins. In the absence of selection by interferon, SIV$_{AGM}$ or SIV$_{SMM}$ may, in theory, develop

any level of sensitivity to IFITM proteins. It is therefore not a surprise that SIV$_{AGM}$ is more restricted by IFITM3 compared to SIV$_{SMM}$.

Human IFITM1, 2 and 3 often show different antiviral activities as a result of their sequence divergence (Lu et al., 2011). Given the closer homology between IFITM2 and 3 than to IFITM1, the antiviral spectra of IFITM2 and 3 are better aligned than with IFITM1. This trend is also seen in this study. IFITM1 is a weaker inhibitor of HIV and SIV as compared to IFITM2 and 3.

We successfully cloned agmIFITM1 from COS-7 and Vero cells. We also cloned four agmIFITM3 variants that differ at amino acid positions 22 and 38. No distinct agmIFITM2 was found. Although we cannot completely rule out the possibility that African green
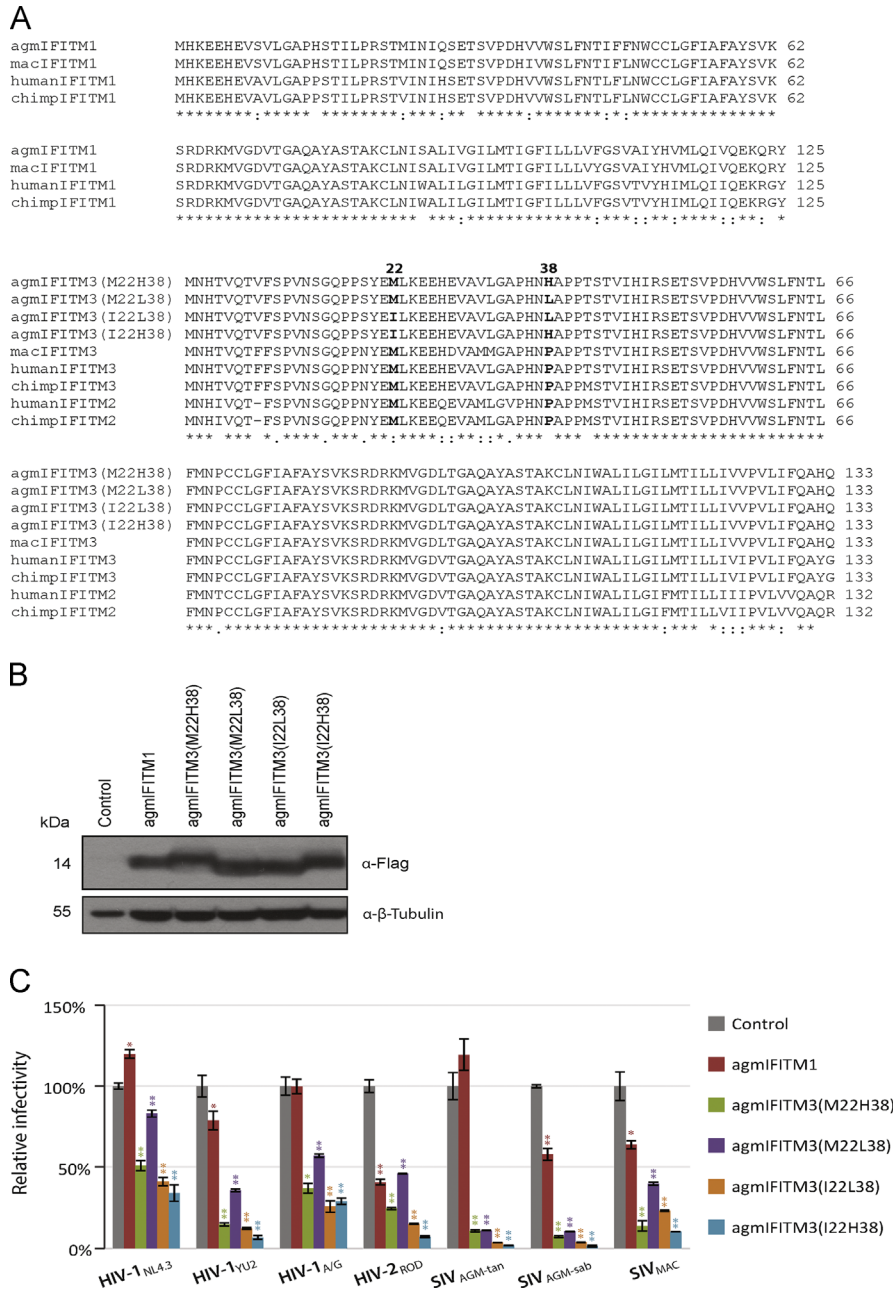
A

```
agmIFITM1     MHKEEHEVSVLGAPHSTILPRSTMINIQSETSVPDHVVWSLFNTIFFNWCCLGFIAFAYSVK 62
macIFITM1     MHKEEHEVSVLGAPHSTILPRSTMINIQSETSVPDHIVWSLFNTIFLNWCCLGFIAFAYSVK 62
humanIFITM1   MHKEEHEVAVLGAPPSTILPRSTVINIHSETSVPDHVVWSLFNTLFLNWCCLGFIAFAYSVK 62
chimpIFITM1   MHKEEHEVAVLGAPPSTILPRSTVINIHSETSVPDHVVWSLFNTLFLNWCCLGFIAFAYSVK 62
              ********:***** *******:***:** *****:*******:*:**************

agmIFITM1     SRDRKMVGDVTGAQAYASTAKCLNISALIVGILMTIGFILLLVFGSVAIYHVMLQIVQEKQRY 125
macIFITM1     SRDRKMVGDVTGAQAYASTAKCLNISALIVGILMTIGFILLLVYGSVAIYHVMLQIVQEKQRY 125
humanIFITM1   SRDRKMVGDVTGAQAYASTAKCLNIWALILGILMTIGFILLLVFGSVTVYHIMLQIIQEKRGY 125
chimpIFITM1   SRDRKMVGDVTGAQAYASTAKCLNIWALILGILMTIGFILLLVFGSVTVYHIMLQIIQEKRGY 125
              *************************** ***:*************:***::**:****::**: *
```

```
                                          22                38
agmIFITM3(M22H38)  MNHTVQTVFSPVNSGQPPSYEMLKEEHEVAVLGAPHNHAPPTSTVIHIRSETSVPDHVVWSLFNTL 66
agmIFITM3(M22L38)  MNHTVQTVFSPVNSGQPPSYEMLKEEHEVAVLGAPHNLAPPTSTVIHIRSETSVPDHVVWSLFNTL 66
agmIFITM3(I22L38)  MNHTVQTVFSPVNSGQPPSYEILKEEHEVAVLGAPHNLAPPTSTVIHIRSETSVPDHVVWSLFNTL 66
agmIFITM3(I22H38)  MNHTVQTVFSPVNSGQPPSYEILKEEHEVAVLGAPHNHAPPTSTVIHIRSETSVPDHVVWSLFNTL 66
macIFITM3          MNHTVQTFFSPVNSGQPPNYEMLKEEHDVAMMGAPHNPAPPTSTVIHIRSETSVPDHVVWSLFNTL 66
humanIFITM3        MNHTVQTFFSPVNSGQPPNYEMLKEEHEVAVLGAPHNPAPPTSTVIHIRSETSVPDHVVWSLFNTL 66
chimpIFITM3        MNHTVQTFFSPVNSGQPPNYEMLKEEHEVAVLGAPHNPAPPMSTVIHIRSETSVPDHVVWSLFNTL 66
humanIFITM2        MNHIVQT-FSPVNSGQPPNYEMLKEEQEVAMLGVPHNPAPPMSTVIHIRSETSVPDHVVWSLFNTL 66
chimpIFITM2        MNHIVQT-FSPVNSGQPPNYEMLKEEQEVAMLGAPHNPAPPTSTVIHIRSETSVPDHVVWSLFNTL 66
                   *** *** *.****.***.**:****:::**::*.*** *** **********************
```

```
agmIFITM3(M22H38)  FMNPCCLGFIAFAYSVKSRDRKMVGDLTGAQAYASTAKCLNIWALILGILMTILLIVVPVLIFQAHQ 133
agmIFITM3(M22L38)  FMNPCCLGFIAFAYSVKSRDRKMVGDLTGAQAYASTAKCLNIWALILGILMTILLIVVPVLIFQAHQ 133
agmIFITM3(I22L38)  FMNPCCLGFIAFAYSVKSRDRKMVGDLTGAQAYASTAKCLNIWALILGILMTILLIVVPVLIFQAHQ 133
agmIFITM3(I22H38)  FMNPCCLGFIAFAYSVKSRDRKMVGDLTGAQAYASTAKCLNIWALILGILMTILLIVVPVLIFQAHQ 133
macIFITM3          FMNPCCLGFIAFAYSVKSRDRKMVGDLTGAQAYASTAKCLNIWALILGILMTILLIVVPVLIFQAHQ 133
humanIFITM3        FMNPCCLGFIAFAYSVKSRDRKMVGDVTGAQAYASTAKCLNIWALILGILMTILLIVIPVLIFQAYG 133
chimpIFITM3        FMNPCCLGFIAFAYSVKSRDRKMVGDVTGAQAYASTAKCLNIWALILGILMTILLIVIPVLIFQAYG 133
humanIFITM2        FMNTCCLGFIAFAYSVKSRDRKMVGDVTGAQAYASTAKCLNIWALILGIFMTILLIIIPVLVVQAQR 132
chimpIFITM2        FMNPCCLGFIAFAYSVKSRDRKMVGDVTGAQAYASTAKCLNIWALILGIFMTILLVIIPVLVVQAQR 132
                   ***.*************************:*************************:*** *::*:***: **
```

B

C

Fig. 5. Inhibition of HIV and SIV by IFITM1 and 3 of African green monkeys. (A) Sequence alignment of agmIFITM1 and 3. IFITM1 and IFITM3 cDNAs were cloned from African green monkey kidney cell lines COS-7 and Vero. Their protein sequences are aligned with orthologs from macaques (mac), humans and chimpanzees (chimp). No distinct IFITM2 was identified. Four agmIFITM3 sequences were found that vary at amino acid positions 22 and 38. (B) TZM-bl cells were stably transduced with agmIFITM1 and four agmIFITM3 variants, then challenged with HIV-1$_{NL4-3}$, HIV-1$_{YU-2}$, HIV-1$_{A/G}$, HIV-2$_{ROD}$, SIV$_{AGM-tan}$, SIV$_{AGM-sab}$ and SIV$_{MAC}$. Results shown are the averages of three independent experiments, with the infectivity in control cells arbitrarily set as 100% for each virus. The pValues were calculated and are presented as * ($p < 0.05$), *** ($p < 0.01$).

monkeys do not have an *ifitm2* gene, no *ifitm2* gene has been described in the macaque genome except for two copies of *ifitm3* genes. In other words, neither of the two copies of macaque *ifitm3* genes has changed significantly enough to become a distinct *ifitm2* gene as seen in humans and chimpanzees. It is possible that in different primate hosts, the *ifitm3* duplicate have undergone different levels of selection and as a result, exhibit different levels of divergence. In some primates, like humans and chimpanzees, one *ifitm3* copy has accumulated enough changes to become a distinct *ifitm2* gene.

HIV and SIV are generally regarded as pH-independent viruses as opposed to pH-dependent viruses such as influenza A viruses that require low pH to accomplish viral membrane fusion (Earp et al., 2005). We further confirmed the pH-independent nature of

SIV$_{AGM}$ by showing its resistance to chloroquine and BafA1 both of which neutralize the pH of late endosomes. We also observed that SIV$_{AGM}$ infection is refractory to dynamin inhibitor dynasore, which suggests that SIV$_{AGM}$ does not need endocytosis to enter cells. Since both SIV$_{AGM}$ and influenza A viruses are potently inhibited by IFITM proteins, it is evident that the routes of virus entry do not necessarily determine the susceptibility of viruses to IFITM restriction. Since the cholesterol-binding compound amphotericin B counters the inhibition of SIV$_{AGM}$ and influenza A virus by IFITMs, IFITM proteins likely utilize the same mechanism to change the membrane fluidity at the virus entry portals and thus block viral membrane fusion.

In conclusion, our study demonstrates that IFITM proteins are able to potently restrict the pH-independent virus such as SIV$_{AGM}$

that does not require endocytosis for its entry. This observation suggests that IFITM proteins do not strictly depend on its localization to late endosomes for its antiviral action. Given the relative closeness of SIV$_{AGM}$ to other IFITM-resistant SIV strains such as SIV$_{MAC}$, there exists an opportunity to identify the viral determinant behind this IFITM resistance phenotype.

Materials and methods

Cell culture

The HEK293T, TZM-bl, COS-7 and Vero cells were grown in Dulbecco's modified Eagle's medium (DMEM) supplemented with 10% fetal bovine serum (Invitrogen) and penicillin/streptomycin (Invitrogen). TZM-bl is an HeLa-derived cell line that expresses CD4, CXCR4 and CCR5 and has a luciferase gene driven by HIV-1 LTR (Wei et al., 2002). C8166 were grown in RPMI1640 medium supplemented with 10% fetal bovine serum and penicillin/streptomycin. Transfection of HEK293T cells was performed with Lipofectamine 2000 (Invitrogen) according to the manufacturer's instructions.

Plasmids

HIV-1$_{YU-2}$ (GenBank M93258), SIV$_{CPZ1.910}$ (GenBank EF394356), SIV$_{AGM-tan}$ (GenBank U58991), SIV$_{AGM-sab}$ (GenBank U04005), and SIV$_{MAC-1A11}$ (GeneBank M76764) proviral clones were obtained through NIH AIDS Reagent Program. HIV-1$_{A/G}$ and HIV-2$_{ROD}$ clones were generously provided by Mark Wainberg. SIV$_{SMM-E543}$ (GenBank U72748) clone was a gift from James Whitney. The human IFITM1, 2 and 3 cDNA sequences were cloned into the retroviral vector pQCXIP as described previously (Lu et al., 2011). shRNA plasmids targeting human ifitm2 and 3 genes were purchased from Sigma and were used to produce lentiviral particles for transduction.

Virus production

To produce HIV-1 (NL4-3, YU2, A/G), HIV-2 (ROD) and SIV (MAC, CPZ, AGM-sab, AGM-tan, SMM), HEK293T cells were transfected with 6 μg of each viral DNA. For the production of BlaM-Vpr-containing viruses, HEK293T cells were transfected with 6 μg of viral plasmid DNA and 2 μg of plasmid DNA encoding the BlaM-Vpr fusion protein. For the production of NL4-3 virus pseudotyped by the VSV G protein, HEK293T cells were transfected with 6 μg of NL4-3(env-) DNA and 0.2 μg of plasmid DNA encoding the G protein of VSV. Forty-eight hours after transfection, culture supernatants were collected and clarified by centrifugation in the CS-6R centrifuge (Beckman Coulter) at 3000 rpm for 30 min at 4 °C. Viruses were aliquoted and stocked at −80 °C. The amounts of viruses were determined by measuring the levels of viral reverse transcriptase activity.

Generation of TZM-bl cells stably expressing IFITM1, IFITM2 or IFITM3

TZM-bl cells were infected with retroviral particles expressing IFITM1, IFITM2 or IFITM3. Cells that stably express IFITMs were selected with puromycin (2 μg/ml). For assessment of IFITM1, IFITM2 and IFITM3 expression by western blot, TZM-bl cells were lysed in the cytobuster buffer (Novagen #71009-4) containing protease inhibitors (Roche #11 836 153 001) for 20 min on ice. Cell lysate was resolved by sodium dodecyl sulfate polyacrylamide gel electrophoresis (SDS-PAGE), blotted onto PVDF (polyvinylidene fluoride) membrane (Roche). IFITMs proteins, containing a Flag tag at their N-termini, were detected using monoclonal antibody against the Flag tag (Sigma #F1804) and horseradish peroxidase conjugated secondary antibodies (GE Healthcare).

Western blotting

Cells were lysed in the cytobuster buffer (Novagen) on ice for 20 min. After a brief spin, cell lysate was collected and mixed with 2 × Laemmli buffer. Proteins were resolved by PAGE and transferred onto the PVDF membrane (Roche). Membranes were blocked for 1 h at room temperature in 4% milk and incubated with primary antibodies overnight at 4 °C. Anti-Flag antibody was purchased from Sigma, anti-IFITM2 and anti-IFITM3 antibodies from ProteinTech. After several washes in 1 × phosphate buffer saline (PBS), membranes were further incubated with horseradish peroxidase-conjugated secondary antibodies (GE Healthcare). Signals were detected by electrochemiluminescence (ECL) and visualized by exposure to a Kodak film.

shRNA silencing of IFITM proteins in TZM-bl and C8166 cells

TZM-bl or C8166 cells were transduced by lentiviral particles allowing the expression of shRNAs against ifitm2 or 3 mRNAs. Three shRNAs were able to deplete both IFITM2 and 3 proteins (TRCN0000057502, TRCN0000118022, TRCN0000118025 from Sigma) and were used in this study. Their sequences are:

shRNA1:CCGGCCTGTTCAACACCCTCTTCTTCTCGAGAAGAAGA-GGGTGTTGAACAGGTTTTTG;
shRNA2:CCGGCCTGTTCAACACCCTCTTCATCTCGAGATGAAGAG-GGTGTTGAACAGGTTTTTG;
shRNA3:CCGGGCTTCATAGCATTCGCCTACTCTCGAGAGTAGGCG-AATGCTATGAAGCTTTTTG.

Twenty-four hours after transduction, cells were treated with or without interferon α2b (IFNα2b) at 1000 U/ml for 24 h, followed by infection with BlaM-Vpr-containing viruses to assess virus entry efficacy.

Entry assay

Viral fusion assay was performed by infecting TZM-bl or C8166 cells as described previously (Lu et al., 2011). In brief, cells were exposed to BlaM-Vpr containing viruses and polybrene (5 μg/ml), and spun for 45 min, 1800 rpm (CS-6R, Beckman Coulter) at 4 °C, then incubated at 37 °C for 2 h. Cells were washed once with CO$_2$ independent medium (Invitrogen), incubated with CCF2-AM containing medium for 1 h at room temperature, washed once and incubated with developing medium at room temperature for 16 h. The following day, cells were washed 2 times in phosphate buffered saline (containing 2% FBS), fixed with 3.7% formaldehyde and analyzed by flow cytometry (BD, Fortessa) to monitor the cleavage of CCF2-AM substrate by BlaM.

Cloning IFITM cDNA from African green monkey cells

COS-7 and Vero cells are both African green monkey kidney cells. They were treated with IFNα2b for 16 h to induce IFITM expression, followed by extraction of total cellular RNA with Trizol (Invitrogen). Purified RNA was reverse transcribed and amplified using a one-step RT-PCR system (Roche) with following primers:

AGM_IFITM1_F1: 5′–CAACAGGGGAAAGCAGGGCTC-3′
AGM_IFITM1_F2: 5′–CAACACTTCTTTCCCCAAAGCCAG-3′
AGM_IFITM1_R1: 5′–GTCATTGTGGACAGGTGTGTGGG-3′
AGM_IFITM1_R2: 5′–CTGTATCTAGGGGCAGGACCAAG-3′
AGM_IFITM2/3_F1: 5′–GGGAAAGGGAGGGCCCACTGAG-3′
AGM_IFITM2/3_F2: 5′–CCCACTAACCCGACCACCGCTG-3′
AGM_IFITM2/3_R1: 5′–GTGTGTGAGGATAAAGGGCTG-3′
AGM_IFITM2/3_R2: 5′–GGGCAGAGCTCCTGGCCTGAATG-3′

These primers were designed as follows. To clone African green monkey IFITM1 (agmIFITM1), we aligned the 5′ and 3′ untranslated regions (UTRs) of the *ifitm*1 genes of human, chimpanzee, pongo, and macaque that are available in Genbank. Two forward and two reverse primers are designed on the basis of the conserved sequences. Primers for agmIFITM2/3 cloning were similarly designed on the basis of the conserved UTRs of human *ifitm*2 and 3, chimpanzee *ifitm*2 and 3, and two macaque *ifitm*3 genes. To amplify IFITM1 or IFITM2/3 cDNA, four RT-PCR reactions were performed using the combinations of the 2 forward and 2 reverse primers. The amplified IFITM DNA fragments were cloned into the pQCXIP retroviral vector (Clontech) between the BamHI and EcoRI restriction sites and sequenced. A Flag tag was added to the N-termini of the agmIFITM proteins and the agmIFITM cDNAs were cloned into pQCXIP for expression.

References

Amini-Bavil-Olyaee, S., Choi, Y.J., Lee, J.H., Shi, M., Huang, I.C., Farzan, M., Jung, J.U., 2013. The antiviral effector IFITM3 disrupts intracellular cholesterol homeostasis to block viral entry. Cell Host Microbe 13 (4), 452–464.

Anafu, A.A., Bowen, C.H., Chin, C.R., Brass, A.L., Holm, G.H., 2013. Interferon inducible transmembrane protein 3 (IFITM3) restricts reovirus cell entry. J. Biol. Chem. 288 (24), 17261–17271.

Bailey, C.C., Huang, I.C., Kam, C., Farzan, M., 2012. Ifitm3 limits the severity of acute influenza in mice. PLoS Pathog. 8 (9), e1002909.

Bailey, C.C., Kondur, H.R., Huang, I.C., Farzan, M., 2013. Interferon-induced transmembrane protein 3 is a type II transmembrane protein. J. Biol. Chem. 288 (45), 32184–32193.

Brass, A.L., Huang, I.C., Benita, Y., John, S.P., Krishnan, M.N., Feeley, E.M., Ryan, B.J., Weyer, J.L., van der Weyden, L., Fikrig, E., Adams, D.J., Xavier, R.J., Farzan, M., Elledge, S.J., 2009. The IFITM proteins mediate cellular resistance to influenza A H1N1 virus, West Nile virus, and dengue virus. Cell 139 (7), 1243–1254.

Chesarino, N.M., McMichael, T.M., Hach, J.C., Yount, J.S., 2014. Phosphorylation of the antiviral protein interferon-inducible transmembrane protein 3 (IFITM3) dually regulates its endocytosis and ubiquitination. J. Biol. Chem. 289 (17), 11986–11992.

Desai, T.M., Marin, M., Chin, C.R., Savidis, G., Brass, A.L., Melikyan, G.B., 2014. IFITM3 restricts influenza A virus entry by blocking the formation of fusion pores following virus-endosome hemifusion. PLoS Pathog. 10 (4), e1004048.

Diamond, M.S., Farzan, M., 2013. The broad-spectrum antiviral functions of IFIT and IFITM proteins. Nat. Rev. Immunol. 13 (1), 46–57.

Earp, L.J., Delos, S.E., Park, H.E., White, J.M., 2005. The many mechanisms of viral membrane fusion proteins. Curr. Top. Microbiol. Immunol. 285, 25–66.

Everitt, A.R., Clare, S., Pertel, T., John, S.P., Wash, R.S., Smith, S.E., Chin, C.R., Feeley, E.M., Sims, J.S., Adams, D.J., Wise, H.M., Kane, L., Goulding, D., Digard, P., Anttila, V., Baillie, J.K., Walsh, T.S., Hume, D.A., Palotie, A., Xue, Y., Colonna, V., Tyler-Smith, C., Dunning, J., Gordon, S.B., Gen, I.I., Investigators, M., Smyth, R.L., Openshaw, P.J., Dougan, G., Brass, A.L., Kellam, P., 2012. IFITM3 restricts the morbidity and mortality associated with influenza. Nature 484 (7395), 519–523.

Feeley, E.M., Sims, J.S., John, S.P., Chin, C.R., Pertel, T., Chen, L.M., Gaiha, G.D., Ryan, B.J., Donis, R.O., Elledge, S.J., Brass, A.L., 2011. IFITM3 inhibits influenza A virus infection by preventing cytosolic entry. PLoS Pathog. 7 (10), e1002337.

Harris, L.D., Tabb, B., Sodora, D.L., Paiardini, M., Klatt, N.R., Douek, D.C., Silvestri, G., Muller-Trutwin, M., Vasile-Pandrea, I., Apetrei, C., Hirsch, V., Lifson, J., Brenchley, J.M., Estes, J.D., 2010. Downregulation of robust acute type I interferon responses distinguishes nonpathogenic simian immunodeficiency virus (SIV) infection of natural hosts from pathogenic SIV infection of rhesus macaques. J. Virol. 84 (15), 7886–7891.

Hickford, D., Frankenberg, S., Shaw, G., Renfree, M.B., 2012. Evolution of vertebrate interferon inducible transmembrane proteins. BMC Genomics 13, 155.

Huang, I.C., Bailey, C.C., Weyer, J.L., Radoshitzky, S.R., Becker, M.M., Chiang, J.J., Brass, A.L., Ahmed, A.A., Chi, X., Dong, L., Longobardi, L.E., Boltz, D., Kuhn, J.H., Elledge, S.J., Bavari, S., Denison, M.R., Choe, H., Farzan, M., 2011. Distinct patterns of IFITM-mediated restriction of filoviruses, SARS coronavirus, and influenza A virus. PLoS Pathog. 7 (1), e1001258.

Jacquelin, B., Petitjean, G., Kunkel, D., Liovat, A.S., Jochems, S.P., Rogers, K.A., Ploquin, M.J., Madec, Y., Barre-Sinoussi, F., Dereuddre-Bosquet, N., Lebon, P., Le Grand, R., Villinger, F., Muller-Trutwin, M., 2014. Innate immune responses and rapid control of inflammation in African green monkeys treated or not with interferon-alpha during primary SIVagm infection. PLoS Pathog. 10 (7), e1004241.

Jia, R., Pan, Q., Ding, S., Rong, L., Liu, S.L., Geng, Y., Qiao, W., Liang, C., 2012. The N-terminal region of IFITM3 modulates its antiviral activity by regulating IFITM3 cellular localization. J. Virol. 86 (24), 13697–13707.

Jia, R., Xu, F., Qian, J., Yao, Y., Miao, C., Zheng, Y.M., Liu, S.L., Guo, F., Geng, Y., Qiao, W., Liang, C., 2014. Identification of an endocytic signal essential for the antiviral action of IFITM3. Cell Microbiol. 16 (7), 1080–1093.

Jiang, D., Weidner, J.M., Qing, M., Pan, X.B., Guo, H., Xu, C., Zhang, X., Birk, A., Chang, J., Shi, P.Y., Block, T.M., Guo, J.T., 2010. Identification of five interferon-induced cellular proteins that inhibit West Nile virus and dengue virus infections. J. Virol. 84 (16), 8332–8341.

Li, K., Markosyan, R.M., Zheng, Y.M., Golfetto, O., Bungart, B., Li, M., Ding, S., He, Y., Liang, C., Lee, J.C., Gratton, E., Cohen, F.S., Liu, S.L., 2013. IFITM proteins restrict viral membrane hemifusion. PLoS Pathog. 9 (1), e1003124.

Lin, T.Y., Chin, C.R., Everitt, A.R., Clare, S., Perreira, J.M., Savidis, G., Aker, A.M., John, S.P., Sarlah, D., Carreira, E.M., Elledge, S.J., Kellam, P., Brass, A.L., 2013. Amphotericin B increases influenza A virus infection by preventing IFITM3-mediated restriction. Cell Rep. 5 (4), 895–908.

Lu, J., Pan, Q., Rong, L., He, W., Liu, S.L., Liang, C., 2011. The IFITM proteins inhibit HIV-1 infection. J. Virol. 85 (5), 2126–2137.

McClure, M.O., Marsh, M., Weiss, R.A., 1988. Human immunodeficiency virus infection of CD4-bearing cells occurs by a pH-independent mechanism. EMBO J. 7 (2), 513–518.

Moffatt, P., Gaumond, M.H., Salois, P., Sellin, K., Bessette, M.C., Godin, E., de Oliveira, P.T., Atkins, G.J., Nanci, A., Thomas, G., 2008. Bril: a novel bone-specific modulator of mineralization. J. Bone Miner. Res. 23 (9), 1497–1508.

Mudhasani, R., Tran, J.P., Retterer, C., Radoshitzky, S.R., Kota, K.P., Altamura, L.A., Smith, J.M., Packard, B.Z., Kuhn, J.H., Costantino, J., Garrison, A.R., Schmaljohn, C.S., Huang, I.C., Farzan, M., Bavari, S., 2013. IFITM-2 and IFITM-3 but not IFITM-1 restrict Rift Valley fever virus. J. Virol. 87 (15), 8451–8464.

Perreira, J.M., Chin, C.R., Feeley, E.M., Brass, A.L., 2013. IFITMs restrict the replication of multiple pathogenic viruses. J. Mol. Biol. 425 (24), 4937–4955.

Sauter, D., Schindler, M., Specht, A., Landford, W.N., Munch, J., Kim, K.A., Votteler, J., Schubert, U., Bibollet-Ruche, F., Keele, B.F., Takehisa, J., Ogando, Y., Ochsenbauer, C., Kappes, J.C., Ayouba, A., Peeters, M., Learn, G.H., Shaw, G., Sharp, P.M., Bieniasz, P., Hahn, B.H., Hatziioannou, T., Kirchhoff, F., 2009. Tetherin-driven adaptation of Vpu and Nef function and the evolution of pandemic and nonpandemic HIV-1 strains. Cell Host Microbe 6 (5), 409–421.

Siegrist, F., Ebeling, M., Certa, U., 2011. The small interferon-induced transmembrane genes and proteins. J. Interf. Cytokine Res. 31 (1), 183–197.

Wakim, L.M., Gupta, N., Mintern, J.D., Villadangos, J.A., 2013. Enhanced survival of lung tissue-resident memory CD8(+) T cells during infection with influenza virus due to selective expression of IFITM3. Nat. Immunol. 14 (3), 238–245.

Warren, C.J., Griffin, L.M., Little, A.S., Huang, I.C., Farzan, M., Pyeon, D., 2014. The antiviral restriction factors IFITM1, 2 and 3 do not inhibit infection of human papillomavirus, cytomegalovirus and adenovirus. PLoS One 9 (5), e96579.

Wei, X., Decker, J.M., Liu, H., Zhang, Z., Arani, R.B., Kilby, J.M., Saag, M.S., Wu, X., Shaw, G.M., Kappes, J.C., 2002. Emergence of resistant human immunodeficiency virus type 1 in patients receiving fusion inhibitor (T-20) monotherapy. Antimicrob. Agents Chemother. 46 (6), 1896–1905.

Weidner, J.M., Jiang, D., Pan, X.B., Chang, J., Block, T.M., Guo, J.T., 2010. Interferon-induced cell membrane proteins, IFITM3 and tetherin, inhibit vesicular stomatitis virus infection via distinct mechanisms. J. Virol. 84 (24), 12646–12657.

Yount, J.S., Karssemeijer, R.A., Hang, H.C., 2012. S-palmitoylation and ubiquitination differentially regulate interferon-induced transmembrane protein 3 (IFITM3)-mediated resistance to influenza virus. J. Biol. Chem. 287 (23), 19631–19641.

Zhang, Y.H., Zhao, Y., Li, N., Peng, Y.C., Giannoulatou, E., Jin, R.H., Yan, H.P., Wu, H., Liu, J.H., Liu, N., Wang, D.Y., Shu, Y.L., Ho, L.P., Kellam, P., McMichael, A., Dong, T., 2013. Interferon-induced transmembrane protein-3 genetic variant rs12252-C is associated with severe influenza in Chinese individuals. Nat. Commun. 4, 1418.

Zhao, X., Guo, F., Liu, F., Cuconati, A., Chang, J., Block, T.M., Guo, J.T., 2014. Interferon induction of IFITM proteins promotes infection by human coronavirus OC43. Proc. Natl. Acad. Sci. USA 111 (18), 6756–6761.